J Arid Land (2023) 15(3): 310–326
https://doi.org/10.1007/s40333-023-0010-y

Science Press Springer-Verlag

Analysis of morphological characteristics of gravels based on digital image processing technology and self-organizing map

XU Tao[1,2], YU Huan[1*], QIU Xia[3], KONG Bo[4], XIANG Qing[1], XU Xiaoyu[5,6], FU Hao[7]

[1] College of Earth Science, Chengdu University of Technology, Chengdu 610059, China;
[2] Beijing SuperMap Software Co., Ltd., Beijing 100015, China;
[3] Sichuan Real Estate Registration Center, Chengdu 610014, China;
[4] Chengdu Institute of Mountain Land and Disasters, Chinese Academy of Sciences, Chengdu 610041, China;
[5] School of Earth Systems and Sustainability, Southern Illinois University Carbondale, Carbondale, IL 62901, United States of America;
[6] Environmental Resources and Policy, Southern Illinois University Carbondale, Carbondale, IL 62901, United States of America;
[7] Sichuan Institute of Land and Space Ecological Restoration and Geohazard Prevention, Chengdu 610081, China

Abstract: A comprehensive understanding of spatial distribution and clustering patterns of gravels is of great significance for ecological restoration and monitoring. However, traditional methods for studying gravels are low-efficiency and have many errors. This study researched the spatial distribution and cluster characteristics of gravels based on digital image processing technology combined with a self-organizing map (SOM) and multivariate statistical methods in the grassland of northern Tibetan Plateau. Moreover, the correlation of morphological parameters of gravels between different cluster groups and the environmental factors affecting gravel distribution were analyzed. The results showed that the morphological characteristics of gravels in northern region (cluster C) and southern region (cluster B) of the Tibetan Plateau were similar, with a low gravel coverage, small gravel diameter, and elongated shape. These regions were mainly distributed in high mountainous areas with large topographic relief. The central region (cluster A) has high coverage of gravels with a larger diameter, mainly distributed in high-altitude plains with smaller undulation. Principal component analysis (PCA) results showed that the gravel distribution of cluster A may be mainly affected by vegetation, while those in clusters B and C could be mainly affected by topography, climate, and soil. The study confirmed that the combination of digital image processing technology and SOM could effectively analyzed the spatial distribution characteristics of gravels, providing a new mode for gravel research.

Keywords: self-organizing map; digital image processing; morphological characteristics; multivariate statistical method; environmental monitoring

Citation: XU Tao, YU Huan, QIU Xia, KONG Bo, XIANG Qing, XU Xiaoyu, FU Hao. 2023. Analysis of morphological characteristics of gravels based on digital image processing technology and self-organizing map. Journal of Arid Land, 15(3): 310–326. https://doi.org/10.1007/s40333-023-0010-y

1 Introduction

Gravel is a comprehensive product of various hydrological and erosion processes, indicating degradation levels in grasslands, soils, and ecosystems (Gao et al., 2013). Soil in northern Tibetan

*Corresponding author: YU Huan (E-mail: yuhuan0622@126.com)
Received 2022-11-17; revised 2023-02-07; accepted 2023-02-22

Plateau is rougher compared with those in other regions of China due to its late formation of geological structure and high abundance of gravels. The presence of gravels will change the surface roughness, which then affects soil infiltration and runoff, and significantly impacts soil hydrothermal processes and vegetation growth (Dong et al., 2004; Yang et al., 2009). Spatial distribution pattern of gravels also determines a variety of important ecological and geomorphological processes, including the distribution of vegetation and animal species (Okin and Painter, 2003; Yamanaka et al., 2004). Therefore, in the study of dynamic monitoring of ecological environment in northern Tibetan Plateau, gravel must be considered as a significant factor that cannot be ignored.

Analyzing the differentiation rule of morphological characteristics of gravels and clarifying the basic relationship between gravels and ecological environment are the basis and premise for reflecting ecological indicators through gravels (Ferguson et al., 2011; Li et al., 2017; Zhang et al., 2021). Therefore, more and more researchers have been analyzing the relationship between morphological characteristics of gravels and environmental factors (Gurnell et al., 2008; Li et al., 2021; Cui et al., 2022). However, current research on gravels primarily focused on the formation mechanism (Guidetti and Boero, 2004), information extraction (David et al., 2005; Duboc et al., 2022), dynamic evolution (Guo et al., 2023), driving mechanisms (Guo et al., 2022a, b), and dynamic monitoring of spatiotemporal changes using remote sensing (Karnieli and Cierniewski, 2001; Wu et al., 2009) with few reports on the clustering of morphological characteristics of gravels in plateau.

Northern Tibetan Plateau is rich in grassland resources, but is also considered as an ecologically fragile area. The region is prone to natural disasters, such as freeze-thaw erosion, water erosion, and wind erosion, which cause an increase in the presence of gravels over time. Studies have shown that the size, shape, coverage, content, and spatial distribution of gravels can significantly affect soil physical properties (Epstein et al., 1996), water movement (Zhan et al., 2017), carbon storage (Nrpa et al., 2019), and nutrient cycling (Lai et al., 2022). These factors have great effects on estimating the process of geomorphic formation (Okin and Painter, 2003), the biomass and net primary productivity of grassland (Reigner and Phillips, 1964; Brouwer and Anderson, 2000), and soil water content (Russo, 1983). Moreover, due to the influence of natural and human activities, the characteristics of gravels often exhibit regularity in spatial distribution (Chen et al., 2020). Clarifying the regularity of gravel clustering is of great significance for the zoning management of ecological environment in northern Tibetan Plateau. Therefore, studying the morphological characteristics and clustering trends of gravels on the surface of the Tibetan Plateau can provide alternative way of thinking the dynamic monitoring of ecological environment in northern Tibetan Plateau, and also provide a theoretical basis for maintaining the healthy and sustainable development of grassland in plateau. However, on the one hand, previous studies of morphological characteristics of gravels primarily used visual estimation and field measurement with low efficiency and large error (Al-Farraj and Harvey, 2000; Adelsberger et al., 2009; Rostagno and Degorgue, 2011). On the other hand, mathematical analysis (such as principal component analysis (PCA), correlation analysis, factor analysis, discriminant analysis, and cluster analysis) have been widely used in the study of gravels (Li et al., 2007; Chen et al., 2011; Gonga et al., 2018).

Digital image processing technology can be used to calculate particle size, coverage, and feature parameters (Ibbeken and Schleyer, 1986). This method can produce almost complete sieving equivalences, thus greatly improving the accuracy of gravel feature extraction. The self-organizing map (SOM) is an unsupervised learning algorithm for clustering and high-dimensional visualization of complex data with nonlinear relationships (Nakagawa et al., 2020). The SOM adopts a competitive learning method in the absence of supervision and training algorithms. The primary objective of learning process is to choose the best matching neuron and update the weight vector adaptively through iteration. Learning results in the formation of a cluster area near the best-matched neurons. Finally, effective clustering and forecast are achieved through intuitive and informative map visualization, which greatly enhances our understanding of gravel characteristic differentiation (Dai et al., 2018; Kim et al., 2020; Guo et al., 2022). This

study combines digital image processing technology with SOM, visualizes SOM classification results through geographic information system (GIS) technology, and synthesizes Pearson correlation coefficient and PCA to determine the environmental factors affecting gravel distribution. Therefore, the objectives of this study are to (1) extract the characteristic parameters of gravels based on digital image processing technology and reveal its spatial distribution pattern; (2) cluster the morphological characteristics of gravels by SOM and analyze differences between clusters; and (3) identify environmental factors that affect gravel distribution through correlation analysis and PCA.

2 Materials and methods

2.1 Study area

Northern Tibetan Plateau is an important ecological security barrier in China. Due to its geological structure, gravels are abundant in the soil. The Naqu City is selected as the study area (Fig. 1a). The elevation in the area is above 4100 m a.s.l., with a high degree of terrain fluctuation (Fig. 1b). The climate is arid, with an annual sunshine duration exceeding 2886 h, an average annual temperature below 0°C, and average precipitation of about 400 mm, with no absolute frost-free period. The vegetation is diverse, with alpine meadows as the dominant type and *Carex* steppe as the secondary type (Guo et al., 2018; Liu et al., 2021). Soil types are complex and diverse. The main grassland types include subalpine meadow, alpine meadow, alpine grassland, and alpine desert grassland. Among them, the development of alpine meadow occurs in local plateau with a sub-humid climate (Hao et al., 2020). The humus layer is thick and sticky, with many gravels. Data processing is shown in Figure 1b.

2.2 Data collection and extraction of gravels

The sampling was conducted in July 2019. During the field investigation, we selected 16 points with significant morphological characteristics of gravels based on factors such as safety and accessibility. Each point with an area of 30 m×30 m and comprised four quadrats of 0.5 m×0.5 m, yielding a total of 64 quadrats. The geographic information was recorded for each sample, such as altitude, particle size, and coverage, and high definition images of the samples were taken by a digital camera. In order to avoid the difficulty in obtaining clear gravel shapes due to abnormal changes in the photos, we used standard lenses and small apertures for shooting. During the shooting process, a clearly visible millimeter scale was placed correspondingly. The camera was kept vertically at a height of 1.0–1.5 m above the ground, depending on the size of surface gravels, to ensure the digital images covered a sufficient area and gravels. The open-source software, ImageJ, was used to process the captured samples. The software's Trainable Weka Segmentation plug-in can realize automatic gravel segmentation based on machine learning and extract the gravel information from field samples. Subsequently, various morphological parameters of gravels were calculated (Fig. 1b). The detailed description of each parameter is shown in Table 1 (Balaguer et al., 2010; Mu et al., 2018).

2.3 Inverting spatial distribution of gravels

Studies have shown that surface particle size affects the spectral radiation of remote sensing images. As surface particle size decreases, the ground spectral reflectance increases. Therefore, researchers used remote sensing information to estimate the size of Gobi gravels based on the reflectance spectral characteristics of surface gravels (Salisbury and D'Aria, 1992). In addition, the surface gravels of Gobi is also closely related to geological factors such as digital elevation (Yao et al., 2014). Therefore, the remote sensing spectral values (the first seven bands of OLI (operational land imager) sensor), normalized difference vegetation index (NDVI), green vegetation index (GVI), soil brightness index (SBI), humidity index (HI), normalized difference built-up index (NDBI), clay mineral ratio (CMR), iron oxide ratio (IOR), ferrous minerals ratio (FMR), and geoscience factors (elevation, slope, aspect, topographic relief, and surface roughness)

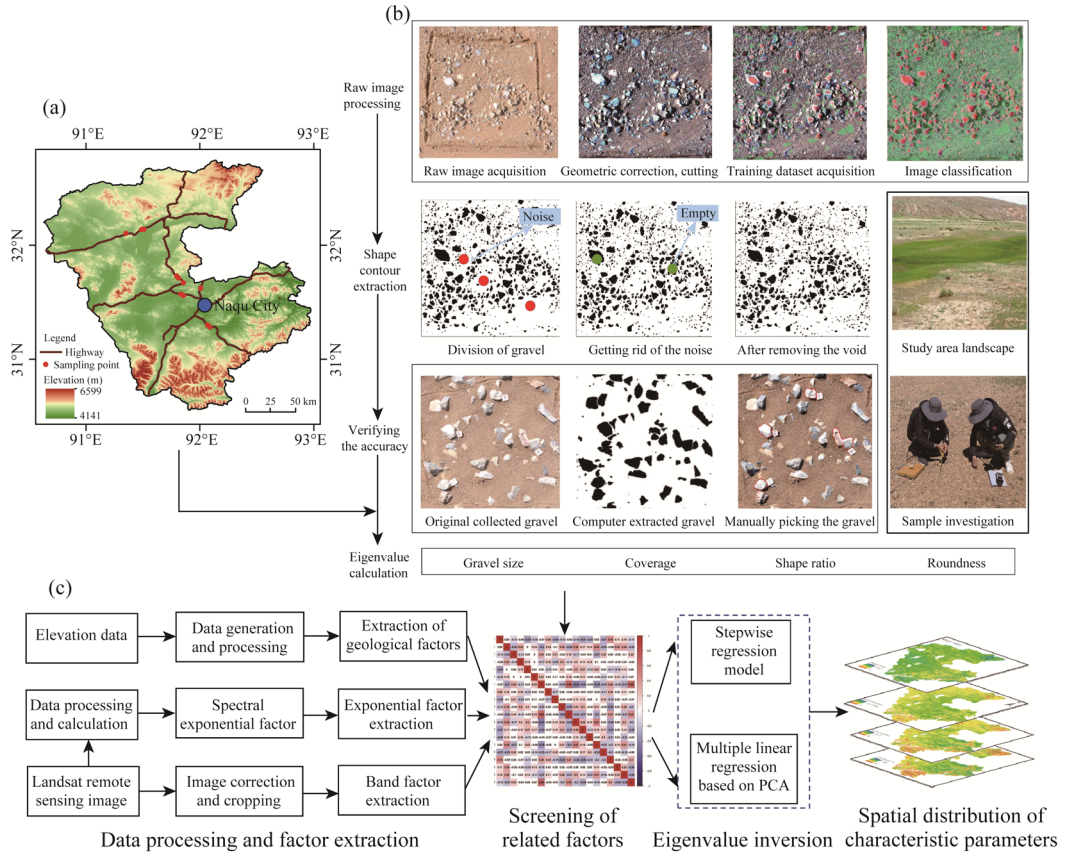

Fig. 1 Research area and data processing. (a), location of sampling points in the study area; (b), extraction morphological characteristics of gravels; (c), inversion morphological characteristics of gravels.

Table 1 Geometric eigenvalue description of gravels

Parameter	Method of calculation	Meaning and unit
Perimeter (L)	Software automatically calculates and counts all gravel edge pixel lengths and converts them to actual lengths	mm
Area (A)	Software automatically calculates and counts the pixel area contained in all gravels and converts it to the actual area	mm^2
Mean gravel size (d_{mean})	$d_{mean} = 2^{\frac{\sum_{i=1}^{i=n} \log_2 F_i}{N}}$	mm
Coverage (C)	$C = \frac{A_p}{A_q} \times 100\%$	Percentage of gravel area (A_p) in the sample to the sample area (A_q); %
Shape ratio (S)	$S = \frac{L_p}{L_m}$	Ratio of long axis (L_p) to short axis (L_m) of gravel, and the greater the value, the more slender the shape
Roundness (G)	$G = \frac{4\Pi A}{L^2}$	Rounding degree of particles, and 1.0 for spherical particles

Note: F_i is the maximum Feret diameter of the i^{th} gravel, N is the number of gravels, and L is length (mm). The methods are referenced from Balaguer et al. (2010) and Mu et al. (2018).

were selected as inversion factors to invert the spatial distribution of gravels (Fig. 1c). The remote sensing data used in this study are Landsat 8 surface reflectance products with a spatial resolution of 30 m and a temporal resolution of 16 d. The images were collected between June and September of 2018, 2019, and 2020, with less than 10% cloud coverage. The images were

preprocessed, including radiometric calibration, atmospheric and geometric correction, mosaic and cutting, and image point and measured point matching, to fulfill the experimental requirements. The data was obtained from the geospatial data cloud platform (http://www.gscloud.cn/).

2.4 Self-organizing map (SOM)

SOM is a two-layer, fully connected neural network with a weight matrix. When analyzing high-dimensional variable problems, relationship between multiple data clusters at a time can't be obtained. SOM can achieve the purpose of dimensionality reduction by generating a two-dimensional topology similar to the original data (Villmann, 1999; Fig. 2a). SOM assigns an initial value to the neuron and then finds the neuron closest to the sample by Euclidean distance for each multi-attribute sample, correcting the weight of neuron. Other neurons near the grid are also corrected synchronously (Fig. 2b). Then, this process is repeated for each sample in training set to complete one SOM learning iteration. The degree of neuron correction is an important basis for measuring whether or not SOM algorithm is convergent. When the convergence condition or the number of iterations is reached, the entire SOM learning will end (Xiang et al., 2022).

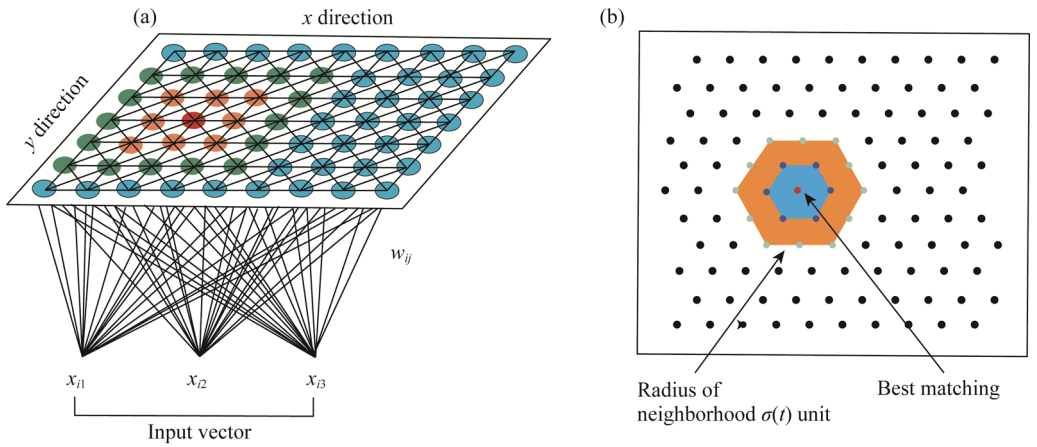

Fig. 2 (a), SOM (self-organizing map) structural diagram chart. x_{i1}, x_{i2} and x_{i3} are the input vectors, and w_{ij} is a weight vector; (b), weight vector adjustment diagram (Zhong et al., 2019).

SOM performs the following three processes (Giraudel and Lek, 2001; Ghaseminezhad and Karami, 2011): (1) competition: for each input vector, the neurons in the network calculate the value of their respective discriminant functions, and the neuron with the maximum value of discriminant functions becomes the winner of competition; (2) cooperation: the winning neuron determines the spatial position of input vector in topological neighborhood and activates the adjacent neurons; and (3) adjustment: with the iteration of algorithm, the best matching unit corresponding to the input vector is locally adjusted to enhance its response to similar input vectors.

SOM neural network method provides a powerful tool for data analysis, classification, and visualization in many researches (Li et al., 2018). It performs a topological preserving transformation from a high-dimensional input data vector space to a low-dimensional output mapping space (Hilker et al., 2009), classifying an input pattern set by finding the optimal set of reference vectors (Wehrens and Buydens, 2007). The specific implementation steps are as follows:

(1) The input space X is N-dimensional vector space $x_i=(x_{i1}, x_{i2},\ldots,x_{iN})$. x_i represents the i^{th} observation sample, and N is the number of parameters to be analyzed.

(2) The output grid size is determined to be m rows and n columns, and $l=m\times n$ grid nodes are randomly generated. Each grid node represents a weight vector, denoted as w_j, where $j=1,2,...,l$.

(3) In the i^{th} iteration, vector $x_i \in X$ is randomly selected as the input vector in the input space.

(4) Calculate the Euclidean distance (d) from x_i to the ownership weight vector, and select the nearest weight vector w_j as the best matching unit.

$$d = \arg \min_{j=1,2,\ldots,l} \| x_i - w_j \|. \quad (1)$$

(5) Updates the weight vector of the best matching unit and neurons in neighborhood with the best matching unit as the center, and applies the update formula.

$$w_j(t+1) = w_j(t) + \eta(t) h_{bj}(t)[x_i - w_j(t)], \quad (2)$$

where $w_j(t+1)$ is the weight vector of j node in $t+1$ iteration process; $\eta(t)$ is the learning speed parameter; $h_{bj}(t)$ is a neighborhood kernel function used to calculate the moving distance of excitation vector around the best matching unit. The Gaussian function is usually selected, that is:

$$h_{bj}(t) = \exp\left[-\frac{d_{bj}^2}{2\sigma(t)^2}\right], \quad (3)$$

where $\sigma(t)$ is the neighborhood radius of the i^{th} iteration process.

(6) Repeat steps 3–5 until the algorithm converges or the iteration reaches the specified number of times, and the iteration process terminates.

3 Results

3.1 Morphological characteristics of gravels

Morphological characteristics of gravels of 16 sample points were extracted and analyzed (Fig. 3a and b). Gravel diameter not only reflects the dynamic conditions of transportation, but also is related to the erosion of external forces such as water and wind. Therefore, study of particle size plays an important role in reflecting the external erosion of northern Tibetan Plateau. The study area consists mostly of fine gravels (4.19–6.27 mm) in 11 sample points, accounting for 68.75% of the sample area and predominantly distributed in central points. The average diameter of gravels in northern and southern points is small, revealing that the erosion effect of external force is weaker in the middle of the study point and stronger in northern and southern points due to higher elevation and the larger topographic relief, which makes gravel diameter smaller. Gravel coverage is higher in the middle of study point and lower in north and south. Among the 16 sample points, gravel coverage of 8 sample points is between 14.78% and 26.15%. This distribution pattern may be related to the larger gravel diameter in the middle of study plots, which creates gaps between the larger gravel diameters and has a blocking and fixing effect on the finer gravel particles, so that they are free from the migration of water flow or wind, resulting in a higher coverage. Shape ratio and roundness are both important parameters reflecting morphological characteristics of gravels. Shape ratio varies from 1.49 to 1.70, and roundness ranges from 0.65 to 0.72, indicating that gravels are mostly near-ellipsoid in shape and elongated. The gravels in northern point are characterized by the largest shape ratio and smallest roundness. It may be due to the nearby accumulation of parent rock after weathering, which influences surface gravel shape by parent rock and contributes to maintaining the state after cracking.

The difference between the maximum and minimum values in the samples reflects the spatial heterogeneity of each parameter (Fig. 3c). Variation of gravel coverage is the largest, ranging from 4.63% to 45.35%. Gravel diameter ranges from 3.46 to 9.46 mm, and the shape ratio varies from 1.43 to 1.84. Variation for roundness is the smallest, ranging from 0.60 to 0.74. The proximity of mean and median values indicates that gravels are concentrated and exhibit a low degree of dispersion.

3.2 Inverting spatial distribution of gravels

Inversion results show spatial distribution of gravels in the study area (Fig. 4a), and the bar graph reflects statistical variation of gravels (Fig. 4b). Inversion diagram clearly illustrates the spatial distribution of gravels, where brown color indicates low value, and green and blue indicate high value. Obviously, high value of gravel diameter is primarily distributed in east, while low value is

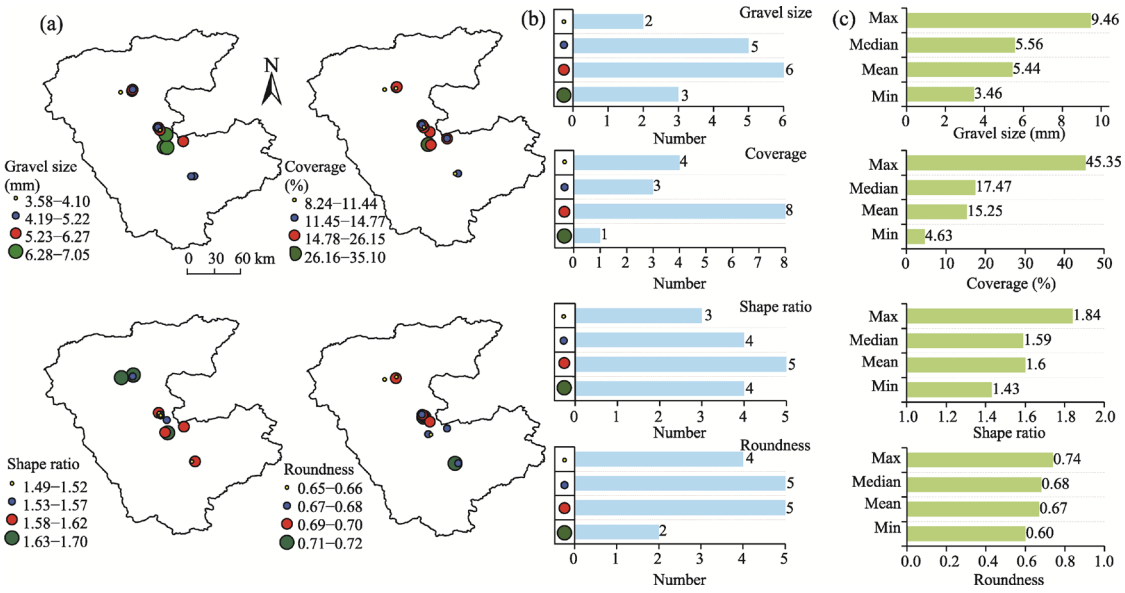

Fig. 3 Morphological characteristic and variation of gravels. (a), spatial distribution of morphological characteristics of gravels in 16 sample points; (b), number of sample points in different grades; (c), morphological variation of gravels.

mostly distributed in north and south. Distribution pattern of gravel coverage is very similar to that of gravel diameter, which further proves the correlation between gravel diameter and gravel coverage. The low value of shape ratio is distributed in southeast, and high value is distributed in north, west, and south. The distribution pattern of roundness is similar to that of shape ratio. According to Figure 4b, gravel diameter ranges from 0.00 to 15.19 mm, with an average of 6.00 mm, most of which are fine gravels. Gravel coverage ranges between 0.00% and 100.00% with an average of 20.42%, shape ratio between 0.00 and 3.63 with an average of 1.54, and roundness between 0.00 and 0.85 with an average of 0.64. However, as seen in the inversion prediction

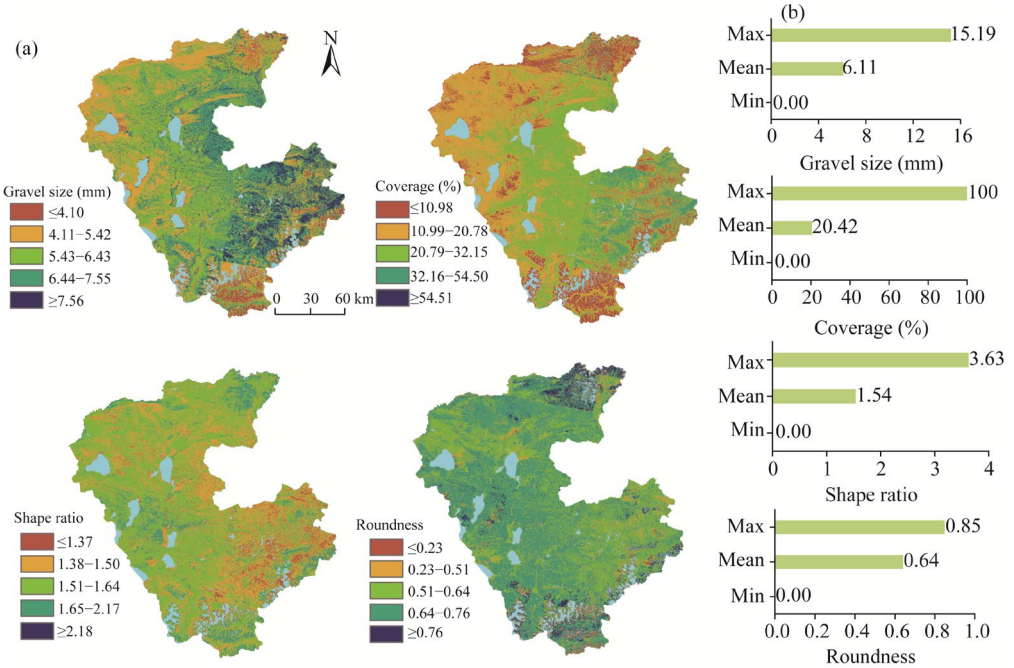

Fig. 4 Inverting spatial distribution of gravels (a) and statistical variation (b)

figure, a few gravels exhibit a shape ratio of less than 1.37 and a roundness of less than 0.51. In general, shape ratio and roundness of gravels change little, and spatial differentiation is weak.

3.3 SOM clustering results

We extracted the gravel characteristic parameter data obtained by inversion according to the hexagonal grid system with a side length of 5 km. A total of 722 datasets of gravel characteristic parameters were extracted and trained as samples for SOM analysis. SOM analysis results are displayed in a U-matrix (Fig. 5a), where different colors represent the distance between each grid node and its adjacent nodes, and each hexagon represents the neuron in the component plane. Nodes in the area with low neighboring distances are similar, while the area with high neighbor distance indicates that the difference between nodes is greater and shows a natural boundary between node clusters. In the figure, gravel diameter and roundness have a high neighborhood distance in the upper and middle parts of the matrix, the upper part of gravel coverage matrix has a high neighborhood distance, and shape ratio has a large difference in the middle of matrix. Parameters obtained by SOM were clustered twice. Firstly, the Davies-Bouldin index (Fig. 5b) was used to calculate the optimal number of clusters. Then, after several iterations (Fig. 5c) and continuous change of the central node of neuron (Fig. 5d), 674 datasets were finally divided into three clusters (Fig. 5e). Weight vector of SOM neuron reveals the contribution of each parameter to the identified clustering, which is the normalized value of gravel characteristic parameters (Fig. 5f). Specifically, cluster A is similar to cluster B, with the gravel diameter and gravel coverage contributing greatly to it. Cluster C has only two neurons, and the contribution value of each parameter is quite different.

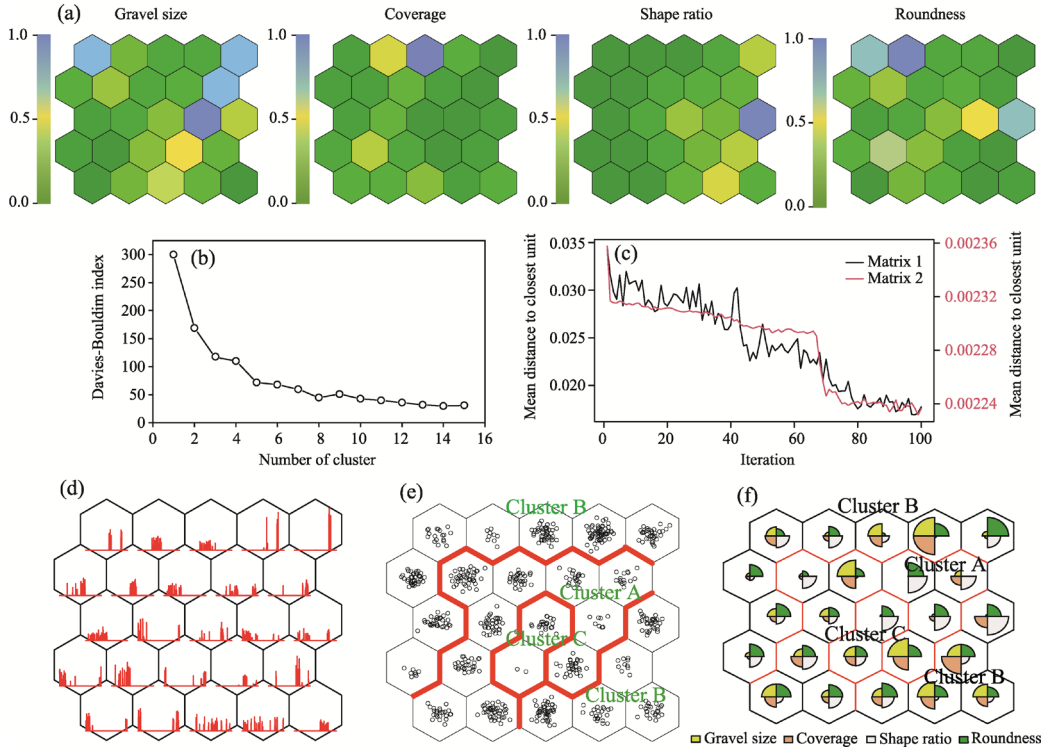

Fig. 5 Result of self-organizing map (SOM). (a), SOM visualization of gravel characteristic parameters, where different colors represent different neighborhood distances; (b), change of Davies-Bouldin index with the optimal number of SOM clusters; (c), SOM iteration process; (d), changing trend of SOM center point in the clustering process; (e), node number and SOM clusters; (f), weight vector distribution.

3.4 Correlation between different clusters

In order to understand the relationship between different clusters, we analyzed characteristic

parameters of gravel dataset (Fig. 6a). It can be seen in cluster A, correlation between gravel diameter and shape ratio is 0.909, which has a strong correlation. Correlation between gravel diameter and gravel coverage is 0.676, and correlations of shape ratio with gravel coverage and roundness are 0.551 and 0.558. Correlations between those parameters of cluster B are lower than that of cluster A, ranging from 0.200 to 0.600, indicating moderate correlations. In cluster C, correlation between gravel diameter and shape ratio is 0.721, and correlation between coverage and roundness is 0.699, showing a strong correlation. In addition, there is also a moderate correlation between shape ratio and roundness. Overall, except for the low correlations among roundness, gravel diameter, and coverage, the correlations between the remaining parameters are above 0.300.

According to the results of SOM clusters, clustering between gravel characteristic parameters is further analyzed (Fig. 6b). From the perspective of clustering, cluster A has the largest number of samples, totaling 389. Sample distribution is more discrete, except for roundness. Average gravel diameter and gravel coverage are higher than the overall mean of sample, the shape ratio is lower than the overall mean of sample, and roundness is roughly equal to the overall mean of sample. The number of samples in cluster B is 275, with a small overall sample fluctuation. Gravel diameter and gravel coverage are lower than the overall mean of sample, and the shape ratio and roundness are higher than the sample mean. Cluster C has the least number of samples, only 58. Sample mean is similar to cluster B, but distribution becomes more discrete.

Fig. 6 Cluster analysis of gravel morphological characteristics. (a), correlation matrix plot of morphological characteristics of gravels. Blue, green, red, and gray fonts represent the correlation between cluster A, cluster B, cluster C and the whole, respectively; blue, green and red dots represent the sample distribution of cluster A, cluster B and cluster C, respectively. *, **, and *** are the significance levels at $P<0.05$, $P<0.01$, and $P<0.001$ levels, respectively. (b), box-whisker plots of cluster A, cluster B and cluster C for morphological characteristics of gravels. The median value is shown as a line within the box. The red dotted line outside the box represents the mean of the samples. Circle is the outlier.

PCA was performed on different clusters (Fig. 7a). For cluster A, the first principal component (PC1) and the second principal component (PC2) explained 66.9% and 22.4% of the variance,

respectively. Therefore, PC1 accounted for 89.3% of the variance. PC1 was closely related to gravel coverage, gravel diameter, shape ratio, and roundness. PC2 was highly correlated with roundness and shape ratio. For cluster B, PC1 and PC2 explained 49.6% and 33.8% of the variance, respectively. PC1 was highly correlated with gravel coverage, gravel diameter size, and shape ratio, and weakly correlated with roundness. Strong correlations with roundness and shape ratio was found in PC2. For cluster C, PC1 and PC2 explained 50.6% and 38.7% of the variance, respectively. PC1 was highly correlated with gravel coverage, roundness, shape ratio, and gravel diameter. PC2 was highly correlated with gravel diameter and shape ratio, and moderately correlated with gravel coverage and roundness. Combination of these first two principal components explained 90.9% of the variance (Fig. 7b). Except for cluster C, which contains part of cluster B, the clustering patterns of gravel parameters are obviously different. Spatial variability of cluster C is significantly higher than those of clusters A and B. Gravel diameter and gravel coverage are closely related to cluster A, and shape ratio and roundness are highly correlated with clusters B and C. Representativeness of different principal components was analyzed from the gravels (Fig. 7c). In different clusters, the most representative factor for PC1 is gravel coverage, while the most representative factor for PC2 is roundness. Geographically, cluster A is mainly distributed in the middle of study area; cluster B is mainly distributed in the south of study area, with occasional occurrences in the central region. Cluster C is mainly distributed in the north of study area (Fig. 7d).

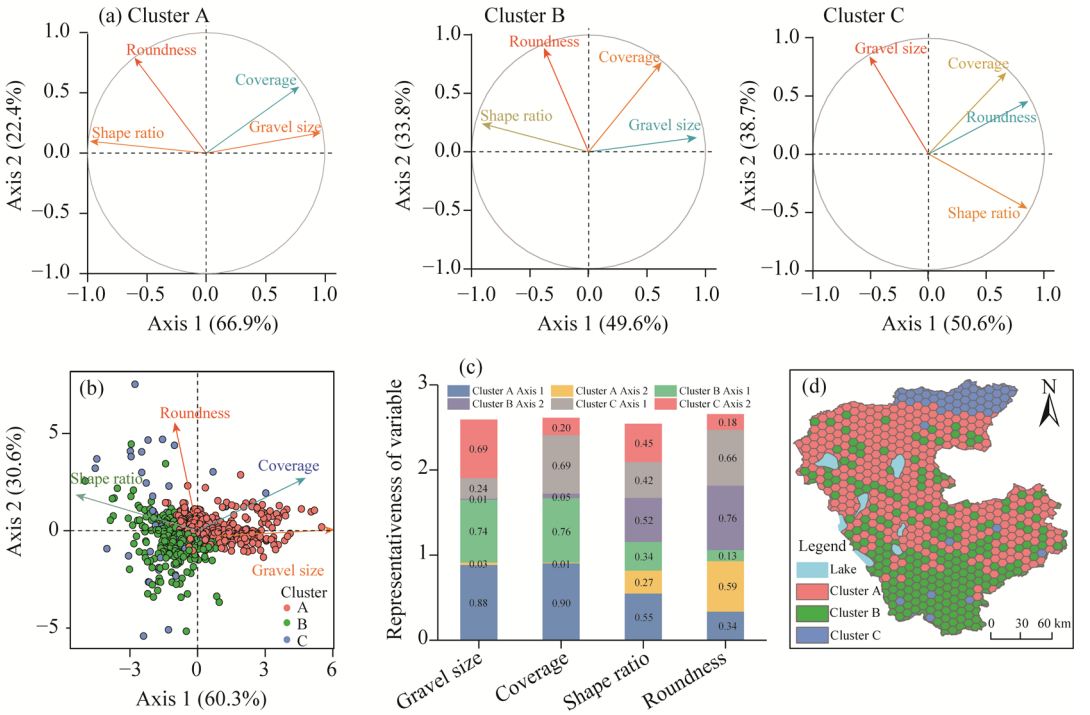

Fig. 7 Principal component analysis (PCA) and spatial distribution of gravels. (a), PCA of different clusters; (b), sample distribution of PCA; (c), representativeness of variable to PCA; (d), spatial distribution of clusters.

4 Discussion

4.1 Advantage of digital image processing technology

Previous studies on quantitative extraction of gravel parameters are mostly based on visual estimation, field measurement, and image analysis (Adelsberger et al., 2009). Visual estimation is usually used to quickly estimate the size and coverage of gravels (Cerda, 2001), but this method is greatly affected by the subjective factors of investigators and lacks accuracy. *In situ*

measurements are used to obtain the average diameter of gravels by sampling them on-site, including screening methods and scale measurements (Al-Farraj et al., 2000). Screening method is limited by the size of sieve and can only obtain the proportion of gravel fixed particle size. Workload of scale measurement is too large and will consume a lot of manpower and material resources. In this paper, characteristic parameters of gravels are extracted by digital image processing technology, and the spatial distribution of gravels is inverted by combining correlation factors. Compared with previous studies, this method has the advantages of non-contact, repeatability, and high precision, which improves the rapidity and accuracy of characteristic parameters of gravels and inversion to a certain extent (Yu et al., 2007). Because morphological characteristics of gravels are often affected by natural and human activities, its spatial distribution has certain regularity. Results of PCA and clustering analysis models are essentially a mixture of dimensions, providing only an initial direction to explain the difference between referenced vectors (Wongravee et al., 2010). As an unsupervised learning algorithm capable of clustering and high-dimensional visualization, SOM can accurately analyze the clustering trend of gravels (Nguyen et al., 2015; Melo et al., 2019). In addition, SOM can effectively capture the spatiotemporal characteristics of nonlinear and complex systems (Mari et al., 2010; Wang et al., 2020). Combination of digital image processing technology and SOM can reveal and clarify the distribution and clustering trend of gravels in northern Tibetan Plateau.

4.2 Influence of environmental variables on gravels

Studies have shown that morphological characteristics of gravels are mainly affected by natural factors such as landform types, land use and cover, and climate, as well as human factors such as construction, farming, and grazing (Ercoli, 2006; Qin et al., 2015). In this paper, the study area is mainly located near Naqu City in northern Tibetan Plateau. The rich grassland resources, diverse landforms, and harsh climatic conditions have important impacts on the morphological characteristics of gravels. Central region (cluster A) has flat terrain, a relatively small temperature difference, and high vegetation cover. Therefore, the main variability of PC1 in cluster A (gravel coverage and gravel diameter) can be considered mainly affected by vegetation. At present, there are two main viewpoints on the influence of vegetation cover and vegetation growth state on the morphological characteristics of gravels. The first one holds that vegetation coverage and growth status are negatively correlated with gravels, as areas with high vegetation cover typically have better soil conditions, smaller gravel diameter, and lower gravel coverage (Grewal et al., 1984; Babalola and Lal, 1997; Ercoli, 2006). Another view is that vegetation cover and vegetation growth status are positively correlated with gravels, because in areas with the high vegetation cover, the erosion of external forces such as water flow and the wind are weak, and dense vegetation has a certain interception effect on gravels, resulting in larger gravel diameter and higher coverage (Jackson et al., 1972; Danalatos et al., 1995; Heisner et al., 2004). In this study, vegetation cover and vegetation growth status are positively correlated with gravels. The terrain in the central region is relatively flat, and the abundant precipitation provides moderate water for vegetation growth (Huang et al., 2013). Additionally, the relatively high temperature affects the physical and chemical properties of the soil by affecting the microbial community and soil enzyme activity in the soil, and ultimately acts on the vegetation, resulting in the higher vegetation cover (Wu et al., 2011; Tripathy et al., 2014). Higher vegetation cover weakens the erosion of external forces on gravels, enhances the interception and accumulation of gravels, and makes the gravel diameter larger and the coverage higher. On the contrary, moderate gravel mulch, on the one hand, helps to improve soil temperature and soil moisture retention, thus providing favorable conditions for root nutrient uptake and being more conducive to plant growth (Pang et al., 2022). On the other hand, it helps to reduce soil erosion and preserve more soil nutrients, thereby increasing vegetation cover and species richness (Figueiredo and Poesen, 1998; Martínez-Zavala and Jordán, 2010). Pearson correlation coefficient confirmed the strong correlation between gravel coverage and gravel diameter, as well as shape ratio and roundness. Therefore, it can be speculated that the total variability of PC1 in cluster A (gravel coverage,

gravel diameter, shape ratio, and roundness) is mainly affected by vegetation. In addition, due to the gap between the surface gravel and the resulting change in aerodynamic roughness, the fine particulate matter transported by the wind is captured and fixed by the gravel gap. Due to the high soil moisture content, the process of coarse particles migrating to the surface caused by cold and heat cycles, dry and wet cycles, will affect the morphological characteristics of gravels.

In contrast, southern region (cluster B) with sparse vegetation is affected by factors such as topography and climate. The main variability of PC1 (gravel coverage) is less affected by vegetation and more affected by topography and climate. Influence of climate on gravels is mainly reflected in temperature differences, precipitation, and wind erosion. Climate conditions in the southern region are relatively harsh with low temperatures, strong sunshine, and high winds throughout the year. Bedrock is strongly eroded by glaciers and cold weathering, and it is easier to form a large number of small gravel-diameter cuttings (Hallet, 1981; Wang et al., 2021). Elevation can be considered a comprehensive manifestation of the combined effects of precipitation and temperature (Marshall and Sklar, 2012). Compared with the central region, the southern region is characterized by a relatively higher elevation and undulating terrain. High, cold, and dry conditions in this environment lead to greater physical weathering in gravels. In addition, hydrothermal conditions at different elevations also have indirect effects on the physical and chemical properties of the soil. As elevation increases, temperature and water decreases, vegetation becomes sparser, and the fragmentation of gravels increases. Some scholars have shown that slope is an important factor affecting the distribution of gravels (Simanton et al., 1994; Poesen et al., 1998; Govers et al., 2006). The greater the slope is, the more intense erosion occurs, resulting in higher gravel fragmentation. Due to the large topographic relief in the southern region, there are mostly fine gravels, and the external force transportation and gravity sedimentation are relatively strong, so gravel coverage and number of gravels are small. Combined with moderate correlation between gravel coverage and gravel diameter size, shape ratio, and roundness in cluster B, it can be inferred that total variability of PC1 in cluster B is affected by topography, climate, and other factors. Correspondingly, northern region can be regarded as a transitional zone between the central and southern regions in terms of topographic relief, climate, and vegetation cover. Therefore, variability of PC1 in cluster C can be inferred to be affected by topography, climate, vegetation, and other factors.

Shape ratio and roundness of gravels are highly correlated with PC2 of clusters A and B, but the influencing factors are different. Due to the flat terrain and large gravel in central region, external force has a limited effect on the transportation of gravels, and the probability of friction and collision between gravels is small. Roundness and shape ratio are mainly affected by vegetation, precipitation, weathering, temperature, and other external forces. Shape of gravels is random, and roundness is more concentrated. Terrain in southern region is undulating, and the gravels are strongly deposited by gravity. Gravels are susceptible to friction and collision, so the roundness is larger, and the distribution is more discrete. Seasonal flooding also occurs in each summer as temperature, melting alpine snow, and rainfall increase (Qian et al., 2014). Top-down flow will cause directional erosion of gravels, which makes a narrower and longer shape of gravels and a larger shape ratio. Northern region (cluster C) can be regarded as a transitional zone between the central and southern regions in terms of topography, climate, and vegetation cover. Therefore, variability of gravels in cluster C can be inferred to be influenced by topography, climate, vegetation, and other factors. However, there are many extreme values due to the influence of remote sensing images during inversion. These extreme values make the sample mean to increase and the distribution discrete.

Human activities may also have an impact on gravel size. In recent years, with the intensification of human activities in northern Tibetan Plateau, natural grasslands in northern Tibetan Plateau have declined, and middle and high-coverage grasslands have changed to low-coverage grassland (Wang et al., 2010). Residential and industrial lands have increased, and the land use types have changed, resulting in a decline in soil and water conservation capacity, and more serious soil damage (Vilmi et al., 2019). Interaction between vegetation degradation and

land desertification has deteriorated the regional ecological environment, resulting in increasing serious external erosion, increasing the quantity of gravels. However, due to the sparse population in the study area, human activities mostly concentrate Naqu City (clusters A and B) in the east, so the impact on gravels is only localized.

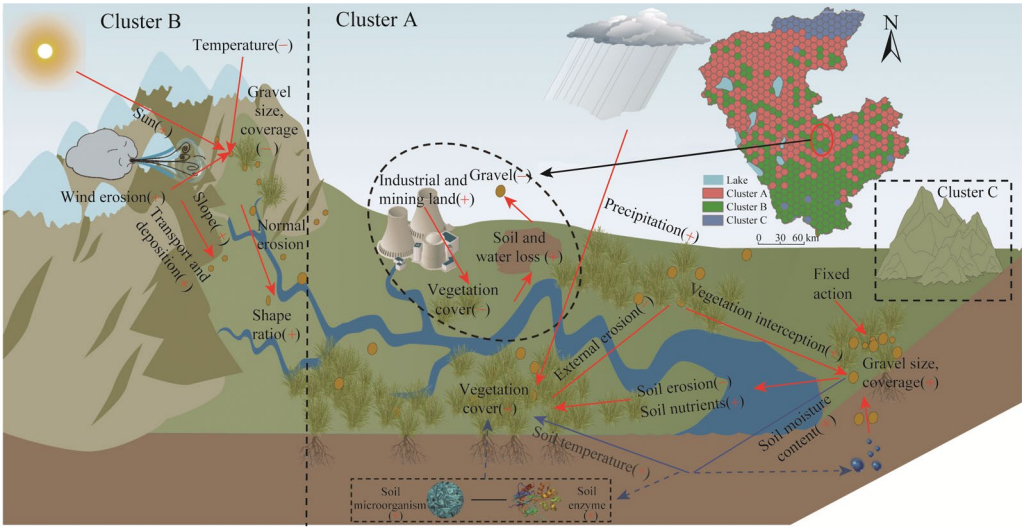

Fig. 8 Influence of environmental variables on gravels in different clusters. + means positive influence, and – means negative influence.

5 Conclusions

In this study, morphological characteristics of gravels in northern Tibetan Plateau were extracted by digital image processing technology, and the gravels were classified by SOM. Spatial gradient of gravels was divided and identified, which clearly showed the distribution and clustering trends of gravels in northern Tibetan Plateau. The results showed that compared with cluster A, cluster B has a smaller gravel diameter, lower coverage, and narrower shape. Mean of each parameter in cluster C is similar to cluster B, but the distribution is more discrete. The reason is that there is more cloud cover in the remote sensing image during inversion, resulting in inversion error and extreme point. In addition, factors affecting the morphological characteristics of gravels were discussed. Cluster A is mainly affected by vegetation; cluster B is mainly affected by terrain and climate, and cluster C is mainly affected by topography, climate, vegetation, and other factors. In this study, SOM combined with traditional multivariate statistical techniques is an effective tool to understand the correlation and clustering trend of gravels. Understanding the relationship between morphological characteristics of gravels and environmental factors will greatly promote the restoration and monitoring of ecological environment in northern Tibetan Plateau.

Acknowledgements

This study was funded by the National Natural Science Foundation of China (41971226, 41871357), the Major Research and Development and Achievement Transformation Projects of Qinghai, China (2022-QY-224), and the Strategic Priority Research Program of the Chinese Academy of Sciences (XDA28110502, XDA19030303).

References

Adelsberger K A, Smith J R. 2009. Desert pavement development and landscape stability on the Eastern Libyan Plateau, Egypt. Geomorphology, 107(3–4): 178–194.

Al-Farraj A, Harvey A M. 2000. Desert pavement characteristics on wadi terrace and alluvial fan surfaces: Wadi Al-Bih, U.A.E. and Oman. Geomorphology, 35(3–4): 279–297.

Babalola O, Lal R. 1997. Subsoil gravel horizon and maize root growth. Plant and Soil, 46(2): 337–346.

Balaguer A, Ruiz L A, Hermosilla T, et al. 2010. Definition of a comprehensive set of texture semivariogram features and their evaluation for object-oriented image classification. Computers and Geosciences, 36(2): 231–240.

Brouwer J, Anderson H. 2000. Water holding capacity of ironstone gravel in a typic plinthoxeralf in southeast Australia. Soil Science Society of America Journal, 64(5): 1603–1608.

Cerdà A. 2001. Effects of rock fragment cover on soil infiltration, interrill runoff and erosion. European Journal of Soil Science, 52(1): 59–68.

Chen H, Liu J, Wang K, et al. 2011. Spatial distribution of rock fragments on steep hillslopes in karst region of northwest Guangxi, China. CATENA, 84(1–2): 21–28.

Chen H, Bai X, Li Y, et al. 2020. The evolution of rocky desertification and its response to land use changes in Wanshan Karst area. Journal of Agricultural Resources and Environment, 37(1): 24–35. (in Chinese)

Cui Z, Yang W S, Cheng Z, et al. 2022. Top-down degradation of alpine meadow in the Qinghai-Tibetan Plateau: Gravelization initiate hillside surface aridity and meadow community disappearance. CATENA, 210: 105933, doi: 10.1016/J.CATENA.2021.105933.

Dai L J, Wang L Q, Li L F, et al. 2018. Multivariate geostatistical analysis and source identification of heavy metals in the sediment of Poyang Lake in China. Science of the Total Environment, 621: 1433–1444.

Danalatos N G, Kosmas C S, Moustakas N C, et al. 1995. Rock fragments IL their impact on soil physical properties and biomass production under Mediterranean conditions. Soil Use and Management, 11(3): 121–126.

David J G, Ian R, Stephen P R, et al. 2005. Automated sizing of coarse-grained sediments: Image-processing procedures. Mathematical Geology, 37(1): 1–28.

Dong Z B, Wang H T, Liu X P, et al. 2004. A wind tunnel investigation of the influences of fetch length on the flux profile of a sand cloud blowing over a gravel surface. Earth Surface Processes and Landforms, 29(13): 1613–1626.

Duboc O, Hernandez M A, Wenzel W W, et al. 2022. Improving the prediction of fertilizer phosphorus availability to plants with simple, but non-standardized extraction techniques. Science of the Total Environment, 806: 150486, doi: 10.1016/j.scitotenv.2021.150486.

Epstein E G, Grant W J, Struchtemeyer R A. 1966. Effects of stones on runoff, erosion, and soil moisture. Soil Science Society of America Journal, 30(5): 638–640.

Ercoli L, Masoni A, Mariotti M. 2006. Dry matter accumulation and remobilization of durum wheat as affected by soil gravel content. Cereal Research Communications, 34(4): 1299–1306.

Ferguson R I, Bloomer D J, Church M. 2011. Evolution of an advancing gravel front: observations from Vedder canal, British Columbia. Earth Surface Processes and Landforms, 36(9): 1172–1182.

Figueiredo T D, Poesen J. 1998. Effects of surface rock fragment characteristics on interrill runoff and erosion of a silty loam soil. Soil and Tillage Research, 46(1–2): 81–85.

Gao Y, Fu S H, Luo L J, et al. 2013. A study on measurement methods of rock fragment cover. Bulletin of Soil and Water Conservation, 33(4): 264–267, 270. (in Chinese)

Ghaseminezhad M H, Karami A. 2011. A novel self-organizing map (SOM) neural network for discrete groups of data clustering. Applied Soft Computing, 11(4): 3771–3778.

Giraudel J L, Lek S. 2001. A comparison of self-organizing map algorithm and some conventional statistical methods for ecological community ordination. Ecological Modelling, 146(1–3): 329–339.

Gonga T, Zhua Y, Shaoa M. 2018. Spatial distribution of caliche nodules in surface soil and their influencing factors in the Liudaogou catchment of the northern Loess Plateau, China. Geoderma, 329: 11–19.

Govers G, Oost KV, Poesen J. 2006. Responses of a semi-arid landscape to human disturbance: A simulation study of the interaction between rock fragment cover, soil erosion and land use change. Geoderma, 133(1–2):19–31.

Grewal S S, Singh K, Dyal S. 1984. Soil profile gravel concentration and its effect on rainfed crop yields. Plant and Soil, 81(1): 75–83.

Guidetti P, Boero F. 2004. Desertification of Mediterranean rocky reefs caused by date-mussel, *Lithophaga lithophaga* (Mollusca: Bivalvia), fishery: Effects on adult and juvenile abundance of a temperate fish. Marine Pollution Bulletin, 48(9/10): 978–982.

Guo B, Kong W H, Jiang L, et al. 2018. Analysis of spatial and temporal changes and its driving mechanism of ecological vulnerability of alpine ecosystem in Qinghai Tibet Plateau. Ecological Science, 37(3): 96–106. (in Chinese)

Guo B, Yang F, Li J L, et al. 2022a. A novel-optimal monitoring index of rocky desertification based on feature space model and red edge indices that derived from sentinel-2 MSI image. Geomatics, Natural Hazards and Risk, 13(1): 1571–1592.

Guo B, Yang F, Fan J F, et al. 2022b. The changes of spatiotemporal pattern of rocky desertification and its dominant driving

factors in typical Karst mountainous areas under the background of global change. Remote Sensing, 14(10): 2351, doi: 10.3390/rs14102351.

Guo B, Yang F, Fan Y W, et al. 2023. The dominant driving factors of rocky desertification and their variations in typical mountainous Karst areas of southwest China in the context of global change. CATENA, 220: 106674, doi: 10.1016/j.catena.2022.106674.

Guo G H, Li K, Zhang D G, et al. 2022. Quantitative source apportionment and associated driving factor identification for soil potential toxicity elements via combining receptor models, SOM, and geo-detector method. Science of the Total Environment, 830, doi: 10.1016/j.scitotenv.2022.154721.

Gurnell A M, Blackall T D, Petts G E. 2008. Characteristics of freshly deposited sand and finer sediments along an island-braided, gravel-bed river: the roles of water, wind and trees. Geomorphology, 99(1–4): 254–269.

Hallet B. 1981. Glacial abrasion and sliding: Their dependence on the debris concentration in basal ice. Annals of Glaciology, 2(1): 23–28.

Hao A H, Xue X, Peng F, et al. 2020. Different vegetation and soil degradation characteristics of a typical grassland in the Qinghai-Tibetan Plateau. Acta Ecologica Sinica, 40(3): 964–975. (in Chinese)

Heisner U, Raber B, Hildebrand E E. 2004. The importance of the soil skeleton for plant-available nutrients in sites of the Southern Black Forest, Germany. European Journal of Forest Research, 123(4): 249–257.

Hilker T, Wulder M A, Coops N C, et al. 2009. A new data fusion model for high spatial- and temporal-resolution mapping of forest disturbance based on Landsat and Modis. Remote Sensing of Environment, 113(8): 1613–1627.

Huang J, Li Z, Zeng G, et al. 2013. Microbial responses to simulated water erosion in relation to organic carbon dynamics on a hilly cropland in subtropical China. Ecological Engineering, 60: 67–75.

Ibbeken H, Schleyer R. 1986. Photo-sieving: A method for grain-size analysis of coarse-grained, unconsolidated bedding surfaces. Earth Surface Processes and Landforms, 11(1): 59–77.

Jackson L P, Hall I V, Aalders L E. 1972. Lowbush blueberry seedling growth as affected by soil type. Canadian Journal of Soil Science, 52(1): 113–115.

Karnieli A, Cierniewski J. 2001. Inferring the roughness of desert rocky surfaces from their bidirectional reflectance data. Advances in Space Research, 28(1): 171–176.

Kim K, Yun S, Yu S, et al. 2020. Geochemical pattern recognitions of deep thermal groundwater in South Korea using selforganizing map: Identified pathways of geochemical reaction and mixing. Journal of Hydrology, 589: 125202, doi: 10.1016/j.jhydrol.2020.125202.

Lai X, Zhu Q, Castellano M J, et al. 2022. Soil rock fragments: Unquantified players in terrestrial carbon and nitrogen cycles. Geoderma, 406: 115530, doi: 10.1016/j.geoderma.2021.115530.

Li H R, Zou X Y, Zhang C L, et al. 2021. Effects of gravel cover on the near-surface airflow field and soil wind erosion. Soil & Tillage Research, 214: 105133, doi: 10.1016/j.still.2021.105133.

Li T, He B, Chen Z, et al. 2017. Effects of gravel on concentrated flow hydraulics and erosion in simulated landslide deposits. CATENA, 156: 197–204.

Li X Y, Contreras S, Solé-Benet A. 2007. Spatial distribution of rock fragments in Dolines: A case study in a semiarid Mediterranean mountain-range (Sierra de Gádor, SE Spain). CATENA, 70(3): 366–374.

Li Z, Bagan H, Yamagata Y. 2018. Analysis of spatiotemporal land cover changes in Inner Mongolia using self-organizing map neural network and grid cells method. Science of the Total Environment, 636: 1180–1191.

Liu F, Liu F G, Zhou Q, et al. 2021. Ecological risk and regional differentiation in the Qinghai-Tibet Plateau. Journal of Natural Resources, 36(12): 3232–3246. (in Chinese)

Mari M, Nadal M, Schuhmacher M, et al. 2010. Application of self organizing maps for PCDD/F pattern recognition of environmental and biological samples to evaluate the impact of a hazardous waste incinerator. Environmental Science & Technology, 44(8): 3162–3168.

Marshall J A, Sklar L S. 2012. Mining soil databases for landscape-scale patterns in the abundance and size distribution of hillslope rock fragments. Earth Surface Processes & Landforms, 37(3): 287–300.

Martínez-Zavala L, Jordán A. 2010. Effect of rock fragment cover on interrill soil erosion from bare soils in Western Andalusia, Spain. Soil Use and Management, 24(1): 108–117.

Melo D S, Gontijo E S, Gontijo D, et al. 2019. Self-organizing maps for evaluation of biogeochemical processes and temporal variations in water quality of subtropical reservoirs. Water Resources Research, 55(12): 10268–10281.

Mu Y, Wang F, Zheng B Y, et al. 2018. McGET: A rapid image-based method to determine the morphological characteristics of gravels on the Gobi desert surface. Geomorphology, 304: 89–98.

Nakagawa K, Yu Z, Berndtsson R, et al. 2020. Temporal characteristics of groundwater chemistry affected by the 2016

Kumamoto earthquake using self-organizing maps. Journal of Hydrology, 582: 124519, doi: 10.1016/j.jhydrol.2019.124519.
Nguyen T T, Kawamura A, Tong T N, et al. 2015. Clustering spatio–seasonal hydrogeochemical data using self-organizing maps for groundwater quality assessment in the Red River Delta, Vietnam. Journal of Hydrology, 522: 661–673.
Nrpa B, Kala B, Ms C, et al. 2019. Lithology and coarse fraction adjusted bulk density estimates for determining total organic carbon stocks in dryland soils. Geoderma, 337: 844–852.
Okin G S, Painter T H. 2003. Effect of grain size on remotely sensed spectral reflectance of sandy desert surfaces. Remote Sensing of Environment, 89(3): 272–280.
Pang B, Ma X X, Hong J T, et al. 2022. Acquisition pattern of nitrogen by microorganisms and plants affected by gravel mulch in a semiarid Tibetan grassland. Science of the Total Environment, 830: 154635, doi: 10.1016/j.scitotenv.2022.154635.
Poesen J W, Wesemael B V, Bunte K, et al. 1998. Variation of rock fragment cover and size along semiarid hillslopes: a case-study from southeast Spain. Geomorphology, 23(2–4): 323–335.
Qian G Q, Dong Z B, Luo W Y, et al. 2014. Gravel morphometric analysis based on digital images of different Gobi surfaces in Northwestern China. Journal of Desert Research, 34(3): 625–633. (in Chinese)
Qin Y, Yi S H, Chen J J, et al. 2015. Effects of gravel on soil and vegetation properties of alpine grassland on the Qinghai-Tibetan Plateau. Ecological Engineering, 74: 351–355.
Reigner I C, Phillips J J. 1964. Variations in bulk density and moisture content within two New Jersey coastal plain soils, lake land and Hurst sands. Soil Science Society of America Journal, 28(2): 287–289.
Rostagno C M, Degorgue G. 2011. Desert pavements as indicators of soil erosion on aridic soils in north-east Patagonia (Argentina). Geomorphology, 134(3–4): 224–231.
Russo D. 1983. Leaching characteristics of a stony desert soil. Soil Science Society of America Journal, 47(3): 431–438.
Salisbury J W, D'Aria D M. 1992. Infrared (8–14 μm) remote sensing of soil particle size. Remote Sensing of Environment, 42(2): 157–165.
Simanton J R, Renard K G, Christiansen C M, et al. 1994. Spatial distribution of surface rock fragments along catenas in semiarid Arizona and Nevada, USA. CATENA, 23(1–2): 29–42.
Tripathy S, Bhattacharyya P, Mohapatra R, et al. 2014. Influence of different fractions of heavy metals on microbial ecophysiological indicators and enzyme activities in century old municipal solid waste amended soil. Ecological Engineering, 70: 25–34.
Villmann T. 1999. Topology preservation in self-organizing maps. Kohonen Maps, 27(2): 279–292.
Vilmi A, Tolonen K T, Karjalainen S M, et al. 2019. Niche position drives interspecific variation in occupancy and abundance in a highly-connected lake system. Ecological Indicators, 99: 159–166.
Wang C P, Huang M T, Zhai P M. 2021. Change in drought conditions and its impacts on vegetation growth over the Tibetan Plateau. Advances in Climate Change Research, 12(3): 333–341.
Wang J S, Zhang X Z, Zhao Y P, et al. 2010. Spatiotemporal pattern of alpine grassland productivity in Qiangtang Plateau. Chinese Journal of Applied Ecology, 21(6): 1400–1404. (in Chinese)
Wang K, Wang P, Zhang R, et al. 2020. Determination of spatiotemporal characteristics of agricultural non-point source pollution of river basins using the dynamic time warping distance. Journal of Hydrology, 583: 124303, doi: 10.1016/j.jhydrol.2019.124303.
Wehrens R, Buydens L. 2007. Self- and super-organizing maps in R: The kohonen package. Journal of Statistical Software, 21(5): 1–19.
Wongravee K, Lloyd G, Silwood C, et al. 2010. Supervised self organization maps for classification and determination of potentially discriminatory variables: Illustrated by application to nuclear magnetic resonance metabolomic profiling. Analytical Chemistry, 82: 628–638.
Wu X D, Zhao L, Fang H B, et al. 2011. Soil enzyme activities in permafrost regions of the western Qinghai-Tibetan Plateau. Soil Science Society of America Journal, 76(4): 1280–1289.
Wu Y Z, Gong P, Liu Q, et al. 2009. Retrieving photometric properties of desert surfaces in China using the Hapke model and MISR data. Remote Sensing of Environment, 113(1): 213–223.
Xiang Q, Yu H, Chu H L, et al. 2022. The potential ecological risk assessment of soil heavy metals using self-organizing map. Science of the Total Environment, 843: 156978, doi: 10.1016/j.scitotenv.2022.156978.
Yamanaka T, Inoue M, Kaihotsu I. 2004. Effects of gravel mulch on water vapor transfer above and below the soil surface. Agricultural Water Management, 67(2): 145–155.
Yang J, Mi R, Liu J. 2009. Variations in soil properties and their effect on subsurface biomass distribution in four alpine meadows of the hinterland of the Tibetan Plateau of China. Environmental Geology, 57(8): 1881–1891.
Yao A D, Cao X Y, Feng Y M. 2014. Remote-sensing model for estimating the size of Gobi surface gravel based on principal

components analysis. Journal of Desert Research, 34(5): 1215–1221. (in Chinese)

Yu Q L, Tang C A, Tang S B. 2007. Digital image based characterization method of rocks heterogeneity and its primary application. Chinese Journal of Rock Mechanics and Engineering, 26(3): 551–559. (in Chinese)

Zhan Z Z, Huang Y H, Jiang F S, et al. 2017. Effects of content and size of gravel on soil permeability of the colluvial deposit in Benggang. Journal of Soil and Water Conservation, 31(3): 85–90, 95. (in Chinese)

Zhang S Q, Jiang H C, Fan J W, et al. 2021. Accumulation of a last deglacial gravel layer at Diexi, Eastern Tibetan Plateau and its possible seismic significance. Frontiers in Earth Science, 9: 797732, doi: 10.3389/FEART.2021.797732.

Zhong H R, Cheng Y H, Lin M X, et al. 2019. Lithology identification of complex carbonate based on SOM and fuzzy recognition. Lithologic Reservoirs, 31(5): 84–91. (in Chinese)